Optics and Lasers in Engineering 78 (2016) 113–120

Contents lists available at ScienceDirect

Optics and Lasers in Engineering

journal homepage: www.elsevier.com/locate/optlaseng

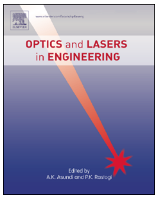

Experimental study on laser microstructures using long pulse

Jing Zhou [a], Hong Shen [b,c,*], Yanqing Pan [b], Xiaohong Ding [a]

[a] *College of Mechanical Engineering, University of Shanghai for Science and Technology, 200093, China*
[b] *School of Mechanical Engineering, Shanghai Jiao Tong University, Shanghai 200240, China*
[c] *State Key Laboratory of Mechanical System and Vibration, Shanghai, 200240, China*

ARTICLE INFO

Article history:
Received 15 August 2015
Received in revised form
17 September 2015
Accepted 22 October 2015

Keywords:
Laser texturing
Long pulse
Surface topography
Ablation volume
Underwater

ABSTRACT

Laser surface texturing has applications in mechanical, medical and electrical industries. Many experiments using the short pulsed laser in air have been performed. In this study, the mechanism of the microstructure produced by using the long pulsed laser from the bump to the dimple is analyzed, in which the surface tension is dominant for the bump shape. The microstructure produced underwater is more regular than the one in air because the spatter of material on the entrance disappears. Due to additional mechanical impacts, liquid-assisted ablation efficiency with a water layer of 0.5 mm shows upto four times higher ablation volume than that in air. More heat dissipation with a thicker liquid layer reduced ablation efficiency.

1. Introduction

Surface texturing is the process of creating microstructures on a surface to reduce and control friction and wear, which extends the lifetime and enhances the behavior of mechanical systems. Therefore, surface texturing has been widely used in mechanical seal rings, piston rings, thrust bearings, sliding bearings, machine tool guide etc. [1–3]. A wide range of texturing techniques is available based on different processes such as micro-indentation [4], electro-erosion [5] and laser texturing [1], among which laser texturing has competitive advantages of localized treated area, fast and clean to the environment, and excellent controllability. Moreover, a laser process can be applied to many materials such as glass, ceramic, polymer and metals.

Etsion et al. [6–8] and Andersson et al. [9] did a lot of work on the laser texturing process. They found that significant improvement in load carrying capacity and wear resistance of mechanical components can be obtained by forming regular microdimples on their surfaces. They also concluded that the laser surface texturing offers the most promising concept compared with other traditional methods. However, their work was mainly focused on the effects of surface texturing on the friction and wear. The analysis of laser microstructure is not discussed in enough depth.

The study of the concave shape generated by the laser is very complicated. A multistep computational model based on COMSOL Multiphysics was developed to investigate the influence of various single-pulse laser energy densities and multiple laser pulses on the temperature history, fluid velocity, crater size, and surface topography [10,11]. Costil et al. [12] investigated the modifications of an aluminum alloy after it had a laser texturation treatment and examined the mechanical and microstructure features of the treated surfaces. However, the bump aspect of the microstructure induced by the pulsed laser is not analyzed.

It is well known that heat accumulation around the laser pulse-affected zone is a big problem in the laser micro-fabrication of materials [13,14] when using long pulse. Heat accumulation can cause defects, ripples, and/or cracks. By adding a water layer onto the target surface, the formation of the melted flow and the re-deposition of ablated material may be avoided. A liquid-confined environment for laser micro-structuring can be achieved in several ways. Examples include ejecting saturated vapor controlled by a heater [15], flowing water film on top of the sample [16], emerging the sample in the water cuvette [17], and depositing a water droplet by using a syringe [18]. Laser structuring underwater by a nanosecond pulse laser has been found to result in reducing substrate defects such as recast layer, dross, cracking and heat damages that are typically found in processing in air [19]. Kang and Welch [20] also studied the effect of liquid thickness on laser ablation efficiency by nanosecond and microsecond pulse lasers. The pulse duration used in these studies is short (mainly nanosecond and microsecond).

In this study, a series of laser texturing were conducted to fabricate microstructures on 304 stainless steel using long pulsed laser (millisecond) in air and underwater. The transformation of

---

* Corresponding author.
E-mail address: sh_0320@sjtu.edu.cn (H. Shen).

http://dx.doi.org/10.1016/j.optlaseng.2015.10.009
0143-8166/© 2015 Elsevier Ltd. All rights reserved.

microstructures from the bump to the dimple is analyzed. The influences of laser power, number of pulses and water layer on the morphology and ablation volume are investigated in detail.

2. Experiments

Laser micro-structuring experiments were performed using an IPG fiber pulsed laser system operating at 1070 nm with maximum power of 1500 W. The laser is operated in the TEM_{00} mode, and the laser beam profile is Gaussian. A convex lens with a focal length of 125 mm is located in a laser cutting head device coupled with the fiber to focus the laser beam on the target surface. The experimental setup in air and underwater is shown in Fig. 1.

The sample used in experiments was AISI 304 stainless steel and the corresponding chemical compositions are given in Table 1. The samples with $50 \times 50 \times 2\ \text{mm}^3$ were cut by a CO_2 laser to prevent from residual stress and deformation. The sample was directly onto a numerically controlled table for the case of processing in air (Fig. 2(a)). In order to better estimate the thickness of the water layer above the sample, a customized wooden box, whose chamber's size being the same as the sample was used to control the water layer through the precise water volume by the measuring cup, as shown in Fig. 2(b). Prior to laser irradiation, distilled water was deposited inside the box for the underwater processing.

The laser processing parameters involved are the laser power (P), heating duration (τ), frequency (f) and the number of laser pulses (n). In order to investigate the effects of laser energy and water layer on the shape of micro-structure, the laser power measured by an Ophir laser powermeter was varied from 300 to 1500 W, while the number of applied pulses was varied from 1 to 35. In this study, the pulse duration and pulse repetition were unchanged, which are 0.2 ms and 50 Hz, respectively. Two thicknesses of water layer above the sample were adopted, which are 0.5 mm and 1 mm (see Table 2).

After the microstructure produced by the laser pulse was cleaned using ultrasonic techniques the profile was examined by utilizing a Keyence KS-1100 3D optical surface profilometer. Ablation volume was quantitatively estimated with three dimensional data of the profile.

3. Mechanism of microstructure formation

Table 3 shows the measurement images of the cross section profile of the microstructure obtained with one laser pulse in air at different energy levels. It can be clearly observed that the topographic feature of the microstructure changes from a sombrero-shaped bump to a bowl-shaped dimple as the increase of the input energy. The transformation of the microstructure can be explained as a result of surface tension driven flow in the molten pool, volumetric forces of the metal liquid and recoil pressure produced by the evaporation. When the laser pulse is fired onto the target, the surface experiences thermo-elastic expansion, melting and vaporization, which depends on the energy employed and the material used.

The energy (Q) that is necessary to melt/evaporate materials is estimated using the following thermodynamic equation,

$$Q = \rho(C_p(T_m - 300) + L_m + C_p(T_b - T_m) + L_b) \tag{1}$$

where ρ is the material density, C_p is the specific heat, T_m and T_b are the melting and vaporization temperatures, respectively, and L_m and L_b are the latent heats of melting and boiling. The thermal properties of 304 stainless steel (see Table 4) used here are assumed to be independent of the temperature.

The pulse energy (E_p) that is necessary to initiate melting/vaporization of the metal can be estimated using the following equations,

$$E_p = QV/A \tag{2}$$

$$V = \frac{1}{3}\pi r^2 L_d \tag{3}$$

$$E_p = P\tau \tag{4}$$

where V is the material volume of melting/vaporization, r is the laser beam radius, A is the absorptivity and L_d is the propagation length of the heat wave over a time span equaling the duration of the pulse τ [22]. L_d is given by:

$$L_d = \sqrt{\alpha\tau} \tag{5}$$

$$\alpha = k/(\rho C_p) \tag{6}$$

where α is the thermal diffusivity and k is the thermal conductivity of the metal. In this study the laser beam radius is 0.25 mm and the coefficient of absorption A is approximately 0.25 and 0.5 at solid and liquid state for 304 stainless steel. The laser power which is required to initiate melting and vaporization can be estimated to be 300 W and 1114 W, respectively. These values seem to agree with the experimental results shown in Table 3.

At the low energy input, the material goes to a molten state. The molten metal flow is governed by the volumetric forces and the surface forces, in which the volumetric forces include the gravity forces made of the classical inertia force and buoyancy

Table 1
304 Stainless Steel Composition (wt%).

Fe	C	Cr	Ni	P	S	Mn
69.928	0.1	18.1	8.4	0.040	0.022	0.31

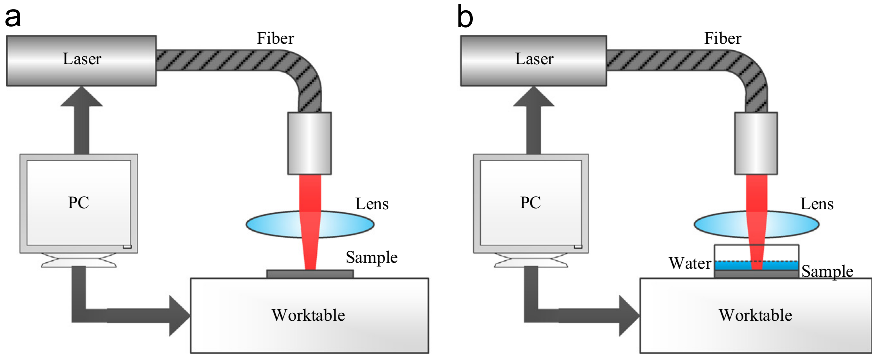

Fig. 1. The schematic of experimental set-up of laser micro-structuring.